STM JOURNALS

Journal of
Nanoscience, Nanoengineering & Applications

ISSN: 2231-1777 (Online)
ISSN: 2321-5194 (Print)
Volume 15, Issue 1, 2025
January–April
DOI (Journal): 10.37591/JoNSNEA

https://journals.stmjournals.com/jonsnea

Research JoNSNEA

Variables Influencing the Reinforcing Effect of Organoclay in Polymer Nanocomposites

Haydar U. Zaman*

Abstract

This study examines how several factors affect the mechanical and thermal characteristics, such as tensile strength, tensile modulus, impact strength, thermal decomposition temperature, and Vicat softening point tests of poly(vinyl chloride)/organoclay nanocomposites. The variables included three different organoclay loading levels, three different screw rotation speeds, and three different plasticizer contents. A co-rotating twin-screw extruder was used to create the poly(vinyl chloride)/organoclay nanocomposite via the melt intercalation process. The properties of the nanocomposite were examined in relation to the impacts of organoclay loading, extruder rotor speed, and plasticizer (dioctyl phthalate) with different concentrations. The clay content of 3 weight percent organoclay showed notable improvements in mechanical parameters, such as tensile strength, tensile modulus, and impact strength, with the maximum mechanical test values generally occurring at 100 rpm. In contrast to the other system and the poly(vinyl chloride)/organoclay system, the addition of a 20-weight percent dioctyl phthalate plasticizer system at 100 rpm resulted in greater mechanical properties. Photographs taken using a transmission electron microscope revealed that during melt mixing, the organoclay was partially exfoliated and intercalated when dioctyl phthalate was present. The thermal stability of the nanocomposites was evaluated using thermogravimetric analysis. The thermogravimetric analysis results demonstrated that the thermal stability of the poly(vinyl chloride) matrix was considerably enhanced by the addition of organoclay.

Keywords: Poly(vinyl chloride), organoclay, nanocomposites, mechanical properties, thermal properties

INTRODUCTION

Over the past ten years, researchers from academia and industry have shown a keen interest in studying polymer/clay nanocomposites [1–2]. When compared to pristine polymers, polymer/clay nanocomposites typically have better mechanical, thermal, flame-retardant, gas-barrier, and other properties because of the clay's nanometer-sized dispersion [3]. A nylon-6 clay nanocomposite, for instance, had a tensile strength of 49% higher, a tensile modulus of 68% higher, and a heat distortion temperature of 87% higher than virgin nylon-6 at 5% clay loading level, while the impact strength remained nearly constant [4]. When creating new nanocomposites, montmorillonite (OMMT), in addition to different fibers and mineral particles, has been a crucial component of successful reinforcement [5]. One of the most popular and extensively utilized nano-scale fillers is montmorillonite. It has the structure of layered silicate and is a member of the dioctahedral smectite group [6]. The mechanical and thermal properties of the polymer matrix are generally

*Author for Correspondence
Haydar U. Zaman
E-mail: haydarzaman07@gmail.com

Assistant Professor, Department of Physics, National University of Bangladesh and Institute of Radiation and Polymer Technology, Bangladesh Atomic Energy Commission, Savar, Dhaka, Bangladesh.

Received date: November 25, 2024
Accepted date: December 22, 2024
Published date: January 04, 2025

Citation: Haydar U. Zaman. Variables Influencing the Reinforcing Effect of Organoclay in Polymer Nanocomposites. Journal of Nanoscience, Nanoengineering & Applications. 2025; 15(1): 55–64p.

improved to the same degree as 30–50 weight percent of micron-sized fillers by the uniform dispersion of 3–5 weight percent of thin clay layers (about 1 nm thick platelets) [7–8]. Typically, the nanocomposite is made of clay that has been biologically altered and a polymer. OMMT, an aluminosilicate mineral with sodium ions in between the clay layers, is the most widely used type of clay. The clay gallery is the name given to this area in between the clay layers. To make this clay compatible with organic polymers, it is typically made hydrophobic by ion-exchanging the sodium ions with an organic phosphonium or ammonium salt. There are three methods for creating nanocomposites: melt blending, solution blending, and in-situ polymerization [9–10]. The most advantageous of them is melt mixing or compounding in a twin screw extruder since it can be produced in large quantities. Numerous polymer-clay nanocomposites, including polyamide 6/clay nanocomposites [11–12], epoxy/clay nanocomposites [13], acrylic polymer/clay nanocomposites [14], and polystyrene/clay nanocomposites [15–16], have been reported based on the same principles.

Because it is inexpensive and has many uses, poly(vinyl chloride) (PVC) is one of the most significant commercial plastics. The thermoplastic with the most uses these days is PVC, along with polyethylenes. It is unquestionably due to its superior mechanical qualities, high additive compatibility, processability, and affordability [17]. PVC still has a lot of issues, including poor thermal stability and brittleness, despite its immense technical and financial significance. PVC undergoes widespread staining, the development of hydrogen chloride gas, and a reduction in its mechanical and physical qualities because of thermal degradation [18]. In certain applications, the usage of PVC and its composites is restricted by these inherent drawbacks. Therefore, to expand the uses of PVC, new PVC goods with excellent qualities and attributes must be developed. In the absence of a plasticizer or stabilizer, PVC will deteriorate during melting processing. For PVC and its copolymers, plasticizers like dioctyl phthalate (DOP) and diisooctyl phthalate (DIOP) are employed to stabilize the processes and provide the final product flexibility. PVC/clay nanocomposites have been studied by several researchers [19]. DOP was used by Trilica et al. as a co-intercalator for PVC and modified clay [20]. Intercalated PVC/clay nanocomposites with enhanced heat stability were created by Wang et al. [21]. The effects of screw rotation speed and the addition of DOP to PVC/organoclay, however, have not yet been reported.

In this work, the dispersibility of the organoclay and the mechanical and thermal properties of PVC/organoclay nanocomposites are evaluated in relation to the screw rotating speed, clay loading level, and the addition of DOP.

EXPERIMENTAL

Materials

Commercial PVC was acquired for this project from Aldrich Chemical Company. With an average molecular weight (M_n) of 99,000 and a weight average molecular weight (M_w) of 233,000, it has an intrinsic viscosity of 1.40 (Vinh 1.40). Cloisite® 30B, also known as MT2EtOH (M: methyl; T: tallow with approximately 65% C18, 30% C16, and 5% C14; EtOH: bis-2-hydroxyethyl), is an organically modified clay that was acquired from Southern Clay Products, Inc. (Austin, TX). Eastman Chemical Company supplied DOP, which was utilized as a plasticizer in PVC paste and as a co-intercalator between PVC and clay to enable the exfoliated structure.

Techniques

Manufacturing of Nanocomposites

Prior to mixing, all the ingredients were dried in an oven set at 80°C for 12 hours at a steady weight before being allowed to cool to room temperature. Before the mixture was melted, all the compounds were combined for five minutes at room temperature. Three distinct weight percentages of clay (1%, 3%, and 5%), as well as pre-weighed amounts of PVC with and without DOP, were used to create the nanocomposites using various combinations of PVC, OMMT, and DOP. Table 1 lists the formulas of the synthesized nanocomposites. PVC/organoclay/DOP nanocomposites were developed in several circumstances. Melt blending in a co-rotating twin-screw extruder (Brabender Plasticorder, model: PLE-331) was then used to make the mixture of PVC and organic modified clay with DOP. The

blending time and processing temperature were set at 10 minutes and 180°C, respectively. The rotor speeds were set at 50, 100, and 150 rpm. A total of 60 g was the controlled sample weight for each blending. Ten minutes later, the Brabender apparatus's mixing chamber was opened, and the resulting mixture was removed. The resulting mixture was compression-molded between two steel plates at 190°C for five minutes while being compressed at 10 MPa in a hot press. At last, the mold was extracted from the plates and the pressure was released. After that, two thick metal blocks were placed at room temperature and allowed to cool to room temperature. To guarantee a consistent film thickness of 1 mm, a template frame was employed. To test the mechanical qualities, the samples were cut into standard sizes and forms in accordance with ASTM D638-91. After that, the samples were placed in plastic bags to await processing and examination.

Table 1. Mixing ratios for different types of PVC/organoclay/DOP nanocomposites.

Case Number of Materials	Sample Code	PVC (wt%)	Organoclay (wt%)	DOP (wt%)	Screw Speed (rpm)
Case A	PVCr1	100	–	–	50
Case B	PVCr2	100	–	–	100
Case C	PVCr3	100	–	–	150
Case D	PVC1r1	99	1	–	50
Case E	PVC1r2	99	1	–	100
Case F	PVC1r3	99	1	–	150
Case G	PVC3r1	97	3	–	50
Case H	PVC3r2	97	3	–	100
Case I	PVC3r3	97	3	–	150
Case J	PVC5r1	95	5	–	50
Case K	PVC5r2	95	5	–	100
Case L	PVC5r3	95	5	–	150
Case M	PVC3D10r1	87	3	10	50
Case N	PVC3D10r2	87	3	10	100
Case O	PVC3D10r3	87	3	10	150
Case P	PVC3D20r1	77	3	20	50
Case Q	PVC3D20r2	77	3	20	100
Case R	PVC3D20r3	77	3	20	150
Case S	PVC3D30r1	67	3	30	50
Case T	PVC3D30r2	67	3	30	100
Case U	PVC3D30r3	67	3	30	150

Transmission Electron Microscopy (TEM)

Using TEM (TEM: JEM 2010 F) and an acceleration voltage of 200 kV, the morphology of the PVC/clay nanocomposites was examined. Using a diamond knife and an ultramicrotome (Ultracut-1, Bright Instrument Company Limited, UK) in a liquid nitrogen environment, a 70 nm ultra-thin film of the composite was created.

Determining Mechanical Properties

The mechanical characteristics of PVC and PVC/clay nanocomposites were examined in terms of notched impact strength, tensile modulus, and tensile strength. Samples of standard specimens were taken from the compression-molded sheet and conditioned for 24 hours at 25 ± 2°C and 50 ± 5% relative humidity. On a screw-driven universal testing machine (Instron 4466) with mechanical grips and a 10 kN electronic load cell, the tensile tests were measured in accordance with ASTM regulations. The speed of the crosshead was 30 mm/min. To get an average value, each measurement was made five times. An XCJ-40 Charpy impact tester was used to measure notch impact strength. The sample size for the notched impact test was $55 \times 6 \times 4$ mm^3, and the notch depth was one-third of the sample's thickness.

Thermal Evaluation

A thermogravimetric analyzer (Dupont Instruments TGA 2950 analyzer) was used to quantify the sample's weight loss in the process of breakdown. Under an inert nitrogen environment, the samples were heated gradually to 700°C at a rate of 20°C per minute. According to ASTM D 1525, the Vicat softening test was conducted using a Vicat softening tester (Prolific manufacture, Noida, U.P. India). To lower the needle rod so that it rests on the specimen's surface, the sample is placed on a specimen support. For even heat transfer, the bath's temperature was raised at a pace of 50°C per hour while stirring continuously. The Vicat softening temperature was determined by measuring the temperature at which the needle penetrates 1 mm.

RESULTS AND DISCUSSION

Dispersion of Nanofillers

The mechanical properties of the composites can be significantly impacted by the filler's distribution inside the polymer matrix. The dispersion status of clay layers can be readily observed via TEM. The TEM micrographs of the PVC/clay and PVC/clay/DOP nanocomposites are displayed in Figure 1. The figures in the upper section show the quality of distributive mixing and are low magnification (scale bar: 1 nm). To assess the degree of intercalation or exfoliation of the clay platelets in the polymer matrix, the bottom section figures are highly magnified (scale bar: 200 nm). Figure 1 makes it evident that the clay is evenly distributed throughout the PVC matrix. However, a few tiny black spots (black arrow) can be a sign of certain clay particles that are not evenly distributed (Figure 1(a–b)). Additionally, the PVC matrix shows a far more uniform dispersion when DOP is present than when raw clay is used (Figure 1(c–d)). Adding DOP as a plasticizer allows for good dispersion and acts as a co-intercalator between clay and PVC, making the exfoliated structure possible. In the PVC/clay nanocomposites high magnification micrographs in cases G and H, there are sizable clay agglomerations that are greater than those of the PVC/clay/DOP nanocomposites in cases P and Q. Additionally, there are less clay platelets in the clay stacks in case H made with a screw rotating at 100 rpm than in case G made with a screw rotating at 50 rpm. Because there are fewer clay platelets in the clay stacks in example Q than in case P, this tendency is evident. This indicates that for PVC/clay/DOP nanocomposites, the mechanical properties were better with a screw rotation speed of 100 rpm than with a screw rotation speed of 50 rpm in this investigation.

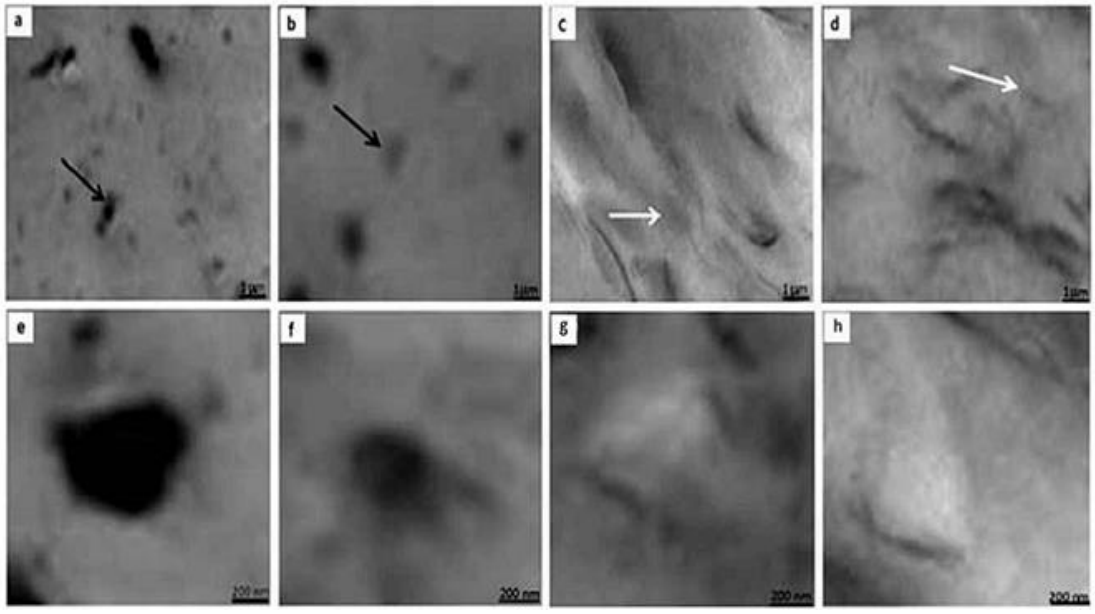

Figure 1. PVC/clay nanocomposites in TEM micrographs: (a) case G; (b) case H; (c) case P; and (d) case Q. With a scale bar of 1 mm, each top micrograph has a low magnification, while each bottom micrograph has a scale bar of 200 nm.

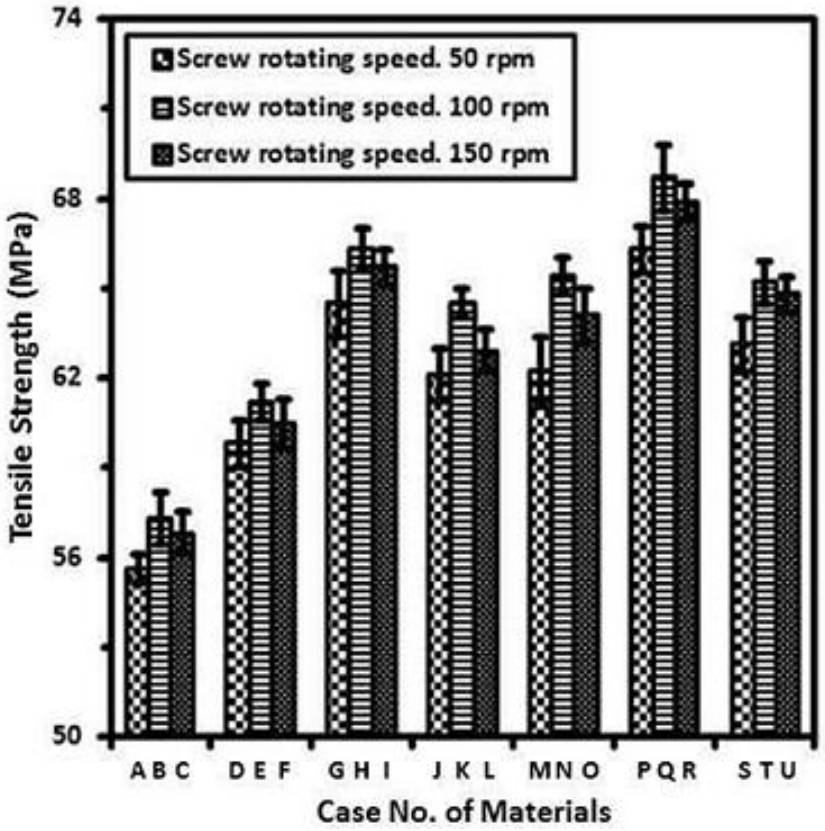

Figure 2. Tensile strength of virgin PVC and different PVC mixes.

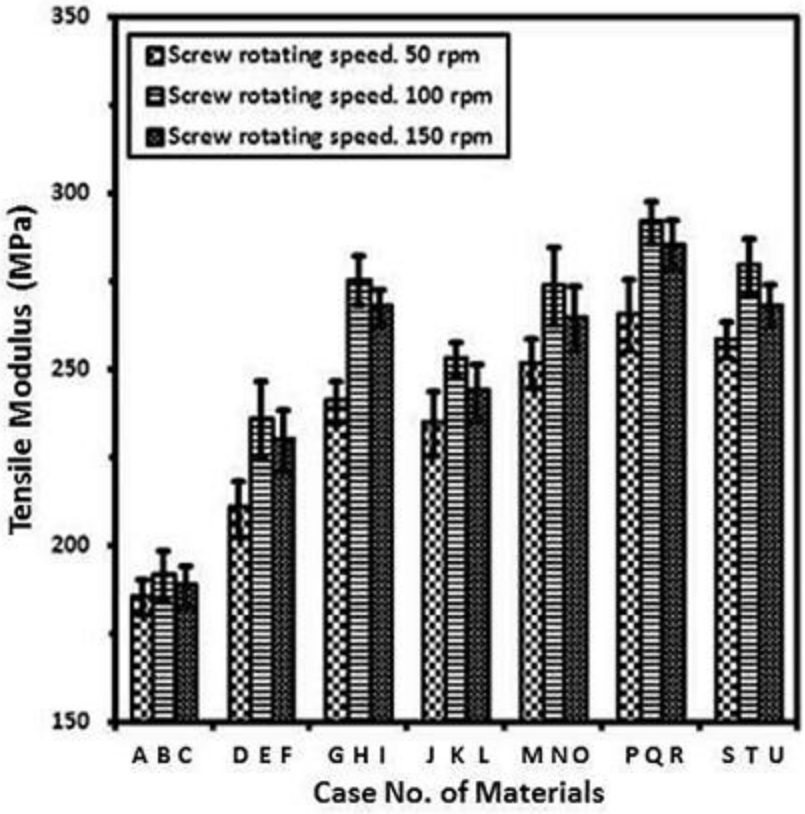

Figure 3. Tensile modulus of virgin PVC and different PVC mixes.

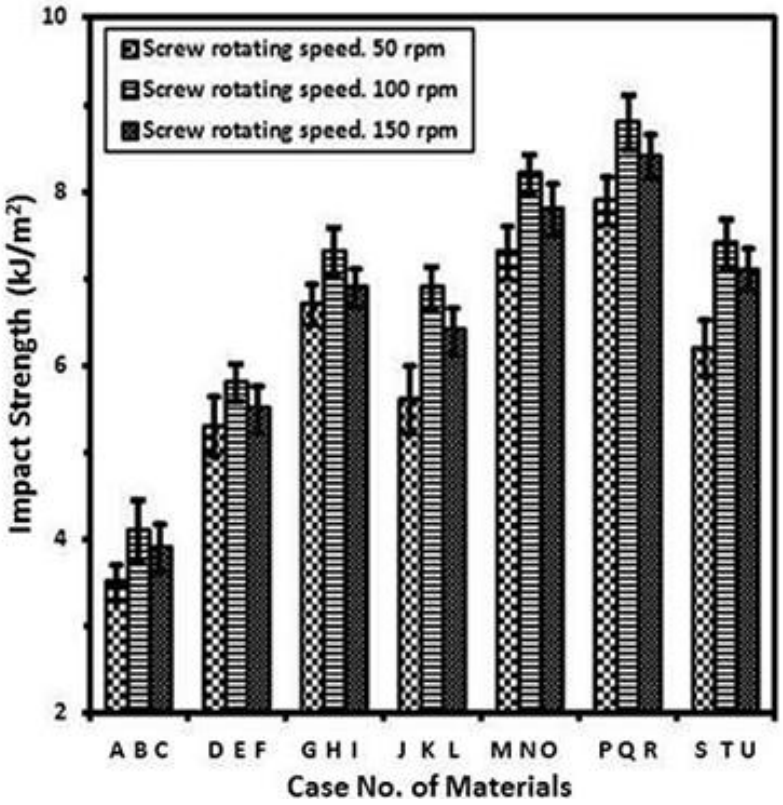

Figure 4. Impact strength of virgin PVC and different PVC mixes.

IMPACT OF LOADING CLAY

Figures 2, 3, and 4 show the tensile and impact characteristics of PVC/organoclay nanocomposites with clay loadings ranging from 1 weight percent to 5 weight percent. Figures 2 and 3 demonstrate that the nanocomposites' tensile strength and tensile modulus increased up to 3% clay loading at a screw speed of 100 rpm (6.8% and 23.2% increment in tensile strength and tensile modulus, respectively, for 1% and 15.7% and 43.8% increment in tensile strength and tensile modulus, respectively, for 3%). Following this, the nanocomposites' tensile strength and modulus decreased when the clay loading was increased to 5% at a screw speed of 100 rpm (12.6% and 32.1% increment in tensile strength and tensile modulus, respectively). At decreased clay loading, the organoclay layers were more evenly distributed and had a positive reinforcing effect. Additionally, it was noted that the filler functions as an active compatibilizer for mixes of binary polymers [22]. The improvement of these qualities decreased with a further increase in organoclay loading (5 weight percent). The findings show that weak areas in the matrix-filler system cause the reinforcing effect to decrease for nanocomposites with increasing clay loading, making them less effective at transferring stress.

Figure 4 displays comparable patterns in the impact strength of PVC-based nanocomposites as a function of clay content. The impact strength of the nanocomposite was approximately 41.5% greater than that of virgin PVC for 1% clay loading at a screw speed of 100 rpm. This increase was further increased by 78% for 3% clay loading and then decreased to 68.3% for 5% clay loading. The increase in impact strength indicated that the significant plastic deformation of the matrix attached to the clay is responsible for the improved resistance to crack propagation. The viscoelastic nature of the interphase causes the circles of matrix around the nanoparticles to agglomerate, which has been shown to be significantly crucial for using failure energy [23–24]. This is obviously a function of the rate of loading. The adverse effect of clay clusters, which results in an uneven dispersion of clay nanolayers in the polymer matrix, is responsible for the reduced impact strength at higher clay loading (5%) levels [25].

THE IMPACT OF SCREW SPEED

The screw speed-dependent tensile strength, modulus, and impact strength are displayed in Figures 2, 3, and 4, respectively. It is evident that as the screw speed increased from 50 to 100 rpm, the mechanical characteristics of the nanocomposites first improved before declining. The best tensile strength was observed at a revolving screw speed of 100 rpm with 3% clay loading, as shown in Figure 2. It appears that better dispersion of nanoclay is encouraged at middle rpm, which enhances tensile strength. Processing at a high speed of 150 rpm in the experiments may result in some structural flaws because of the short residence period. The influence of screw speed on tensile modulus is shown in Figure 3, where the maximum modulus is obtained with 3% clay. Compositions treated at 100 rpm typically exhibit maximal modulus. This maximum might be the consequence of expanding the area of interface produced, which would increase the area available for interactions between the filler and the matrix structures. Because of the short resistance time at high rpm, the degree of dispersion and exfoliation is reduced. The impact of processing speed on material impact resistance is depicted in Figure 4. The dispersion mechanism, residency time and distribution, and shear intensity inside the extruder barrel are all significantly impacted by screw speed. Greater shear intensity is implied by faster rpm, but the barrel's residence duration is shortened. The maximum impact was achieved at 100 rpm with 3% clay loading, as shown in Figure 4. The results are worse when the screw speed is increased to 150 rpm for 3% clay loading. This is because the structure has flaw sites because of the increased shear intensity.

IMPACT OF LOADING PLASTICIZER

Figures 2, 3, and 4 show the effects of plasticizer loading on the nanocomposites' tensile strength, tensile modulus, and impact strength, respectively. According to Figures 2 and 3, the plasticized nanocomposites' tensile strength and tensile modulus increased linearly up to 20% at 100 rpm, surpassing that of virgin PVC by 19.9% and 52.5%, respectively. Following this, the hybrids with a higher DOP content exhibited a negative decline in strength and modulus. The enhancement can be attributed to the reinforcing impact of intercalated nanolayers, which are made possible by strong hydrogen bonding between the oxygen of the silicates and the OH groups of the DOP value group. This increases the nanoclay's inter-gallery space. The reinforced effect of separated nanolayers, which is accomplished by intercalating the invading value group in the nanoclay's inter-gallery space and causing plastic deformation of the polymer matrix, is responsible for the increase in toughness. Because a significant quantity of DOP fraction was added to the hybrid, the nanocomposites displayed a reduced modulus at greater DOP loading. Here, DOP serves as a co-intercalator between clay and PVC, enabling the exfoliated structure to be achieved. This means that when DOP is added to the mixture in the TEM micrographs, the number of clay platelets in the clay stacks of PVC/clay nanocomposites decreases. Figure 4 illustrates comparable patterns in the impact strength of the plasticized nanocomposites as a function of DOP concentrations. It is evident that the impact strength of the nanocomposites increased up to 20% DOP loading at a screw speed of 100 rpm (114.6% increment compared to virgin PVC), after which it decreased when the DOP loading was increased further to 30% at a screw speed of 150 rpm (80.5% increment compared to virgin PVC). Chain entanglement by the intruded DOP macromolecules creating an H-bond with the silicate's oxygen atom inside the clay's inter-gallery region may be the reason for the increase in impact strength. The presence of a significant quantity of DOP fraction, which is what causes the hybrid's decreased impact strength, causes the nanocomposites to exhibit decreased impact strength at increased DOP loading.

Behavior of Thermal Decomposition in Nanocomposites

PVC is recognized to be among the least stable thermoplastics and to break down during melt processing in the absence of a plasticizer or stabilizer [26]. The data for the nanocomposites are provided in Table 2, while the TGA curves for PVC, PVC/OMMT, and PVC/OMMT/DOP nanocomposites are displayed in Figure 5. $T_{0.05}$, the temperature at which 5-weight percent deterioration occurs, and $T_{0.5}$, the temperature at which 50% degradation occurs, are shown in Table 2.

While $T_{0.05}$ represents the beginning of the decline, $T_{0.5}$ also offers some insight into how the degradation progressed. Compared to virgin PVC, the nanocomposites exhibit greater heat stability. The stabilization of PVC may be improved by the addition of inorganic OMMT. Compared to PVC, the nanocomposites' $T_{0.5}$ value is at least 22°C greater. It is unexpected to see that PVC5r2's $T_{0.5}$ and $T_{0.05}$ values are lower than those of PVC3r2 or PVC3D20r2. The poor combination between the polymer and silicates and the aggregation of OMMT may be the cause of this.

To determine the Vicat softening point (VSP), PVC/OMMT nanocomposites with OMMT loading ranging from 0 to 5.0 weight percent were tested. The VSP of PVC and nanocomposites is displayed in Figure 6. It may be found that the VSP temperature of nanocomposites exhibits a steadily increasing trend with increasing clay concentration. The VSP temperature of the PVC/OMMT/100 rpm (PVCOr2) nanocomposite is 93.5°C at a 5-weight percent OMMT concentration, which is 1.2 times higher than that of virgin PVC. There is little doubt that the improved thermal insulation effect of OMMT is the cause of the elevated VSP temperature with increasing OMMT levels. All nanocomposites show higher VSP temperatures than PVC and even higher than the PVCOr2 nanocomposite, and this rise is ascribed to the presence of DOP. PVC/OMMT5wt%/DOP20wt%/100rpm (PVCOD20r2) has a VSP temperature that is 2.6°C higher than PVCOr2, which further supports the idea that the inclusion of DOP has enhanced the adhesion and crosslinking between PVC and DOP.

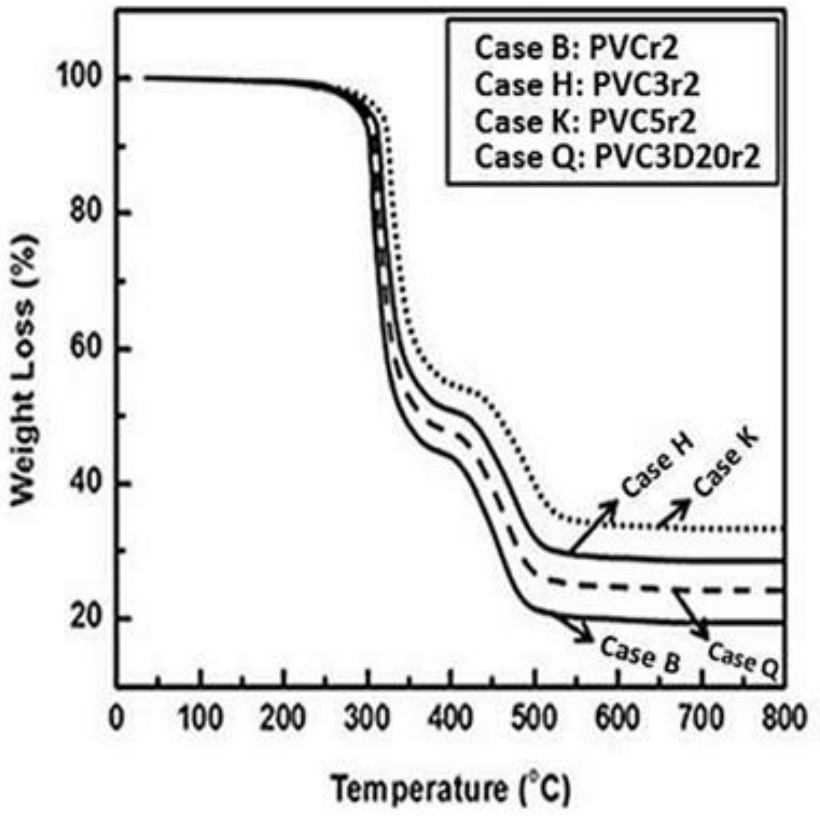

Figure 5. TGA curves of virgin PVC and several PVC/clay nanocomposites: screw speed at 100 rpm.

Table 2. PVC/OMMT nanocomposites' TGA data.

Composites	PVCr2	PVC1r2	PVC1r2	PVC5r2	PVC3D20r2
$T_{0.05}$(°C)	283	290	294	287	298
$T_{0.5}$(°C)	324	351	358	354	361

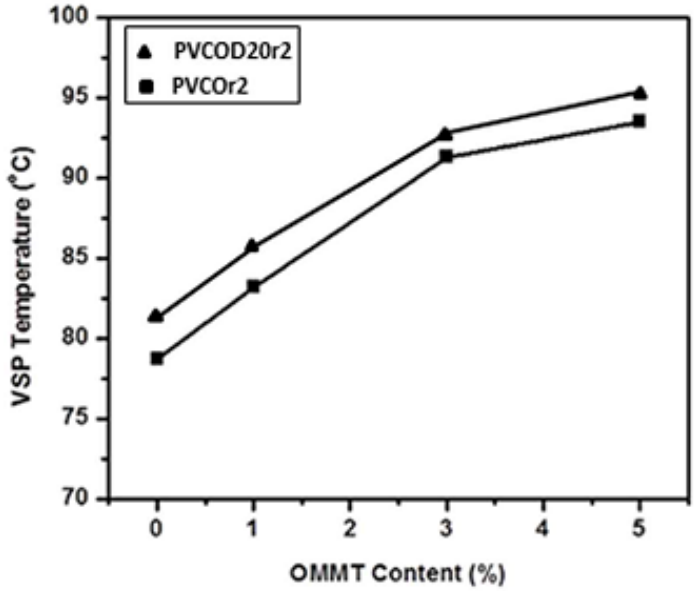

Figure 6. Impact of OMMT concentration on PVC/clay nanocoposites' VSP.

CONCLUSIONS

This article describes the effective preparation of PVC/clay nanocomposites using a melt compounding process with three distinct screw rotation rates (50, 100, and 150 rpm). The clay aggregates in the PVC/Clay/DOP nanocomposites are smaller than those in the PVC/clay nanocomposites, according to TEM images. When the screw rotates at 150 rpm, there are fewer clay platelets in the clay stacks of the PVC/clay and PVC/clay/DOP nanocomposites than when the screw rotates at 100 rpm. With a clay content of 3 weight percent organoclay, mechanical parameters like tensile strength, tensile modulus, and impact strength demonstrate notable improvements. In general, the highest mechanical test values were obtained at a speed of 100 rpm. Higher mechanical qualities were provided by the inclusion of a 20-weight percent DOP plasticizer system operating at 100 rpm as opposed to the PVC/clay system and the other system. Incorporating organoclay enhanced the thermal stability of the nanocomposites.

REFERENCES

1. Maniyar K, Jadhav P, Biradar R, Gawande J. An experimental study of process parameters for nanocomposites. NanoWorld J. 2024;10:209–11.
2. Zaman HU, Hun PD, Khan RA, Yoon KB. Polypropylene/clay nanocomposites: effect of compatibilizers on the morphology, mechanical properties and crystallization behaviors. J Thermoplast Compos Mat. 2014;27:338–49.
3. Pilar C, Suarez M, Jerome R, Hyosung A, Robert C, Nahas, et al. Polymer-clay nanocomposite coatings as efficient, environment-friendly surface pretreatments for aluminum alloy 2024-T3. Electrochimica Acta. 2018;260:73–81.
4. Izadpanah R, Rezaei M, Talebi S. Preparation of cross-linked PVC-g-(St-MA) copolymer/organoclay nanocomposites and investigation of chemical characteristics, morphology, thermal, and mechanical properties. J Thermoplast Compos Mat. 2022;35(2):211–29.
5. Nath AK, Bhaswati S. Electrochemical and thermal properties of polymer-layered silicate nanocomposites for energy storage applications. Polym Polym Compos. 2021;29:547–55.
6. Kausar A. Physical properties of hybrid polymer/clay composites. InHybrid polymer composite materials. Woodhead Publishing; 2017. pp. 115–32.
7. Nilanjal M, Virendra K, Jitendra B, Shovit B, Mazumder S, Lalit V. Layered silicate-polymer nanocomposite coatings via radiation curing process for flame retardant applications. Progr Organ Coat. 2014;77:1443–51.

8. Nekhlaoui S, Abdelaoui H, Raji M. Assessment of thermo-mechanical, dye discoloration, and hygroscopic behavior of hybrid composites based on polypropylene/clay (illite)/TiO_2. Int J Adv Manufact Tech. 2021;113:2615–28.
9. Zaman HU, Beg MDH. Mechanical, thermal, and rheological properties of nano-calcium carbonate/polypropylene composites modified by methacrylic acid. J Thermoplast Compos Mat. 2014;29:189–203.
10. Zaman HU, Hun PD, Khan RA, Yoon KB. Morphology, mechanical, and crystallization behaviors of micro- and nano-ZnO filled polypropylene composites. J Reinf Plast Compos. 2012;31:323–9.
11. Shigemitsu M, Atsushi I, Yoshiharu M, Noritaka K, Yoshiyuki N. Structural characteristics and moisture sorption behavior of nylon-6/clay hybrid films. J Polym Sci Part B Polym Phys. 2002;40:479–87.
12. Wei-Hua Y. The preparation of modified polyamide clay nanocomposite/recycled maleic anhydride polyamide 6 and blending with low density polyethylene for film blowing application. Polym Polym Compos. 2021;29:S631–43.
13. Nóra H, Szabolcs P, Richárd TV, Béla P. Coupling of PMMA to the surface of a layered silicate by intercalative polymerization: processes, structure and properties. Coll Surf A Physicochem Eng Asp. 2020;601:124979.
14. Zina V, Denis Mihaela P, Catalina Gabriela S, Constantin R, Raluca G, Cristian Andi N, et al. The effect of polystyrene blocks content and of type of elastomer blocks on the properties of block copolymer/layered silicate nanocomposites. J Alloy Comp. 2014;616:569–76.
15. Camila R, Ferreira Celso V, Santilli Valérie B, Sandra HP. Relevance of the iron distribution in natural smectite clays for the thermal stability of PMMA–clay nanocomposites. ACS Omega. 2024;34:36579–88.
16. Hadeel A, Hanan A, Ibraheem, Huda Ghazi N, Ala R, Shaker, et al. Enhancing photoirradiation stability: a review on modification of poly(methyl methacrylate). Al-Nahrain J Sci. 2024;27:32–42.
17. Linqin T, Chengyuan S, Yu C, Yunchuan X, Xinyue H, Ziyu Y, et al. Influence of biodegradable polybutylene succinate and non-biodegradable polyvinyl chloride microplastics on anammox sludge: performance evaluation, suppression effect and metagenomic analysis. J Hazard Mat. 2021;401:123337.
18. Margarita M, Sánchez-Valdés S, Sanchez-Espíndola ME, Rivera-López Jesús E. Morphology, mechanical properties, and thermal stability of rigid PVC/clay nanocomposites. Polym Eng Sci. 2011;51:641–6.
19. Trilica J, Kalendova A, Malac Z, Simonik J. Statement of policy release for publication of SPE Conf Paper. May 6–10, 2001. p. 2162.
20. Seyyed B, Abdollahi B, Behnaz B, Fatemeh M, Dorrin Mohtadi H, Zahra M. Clay-reinforced PVC composites and nanocomposites. Heliyon. 2024;10:2405–8440.
21. Nesterov AE, Lipatov YS. Compatibilizing effect of a filler in binary polymer mixtures. Polymer. 1999;40:1347–9.
22. Privalko VP, Shumsky VF, Privalko EG, Karaman VM, Walter R, Friedrich K, et al. Viscoelasticity and flow behavior of irradiation grafted nano-inorganic particle filled polypropylene composites in the melt state. Sci Tech Adv Mat. 2002;3:111–6.
23. Sanghyeon P, Changyub N, Sung-Soo K, Lee Ku K, Hong Gun K, Jin-Hae C, et al. Colorless and transparent polyimide nanocomposites using organically modified montmorillonite and mica. Sci Rep. 2024;14:10670.
24. Neeraj K, Chandra M, Arvind N. An investigative study on the structural, thermal and mechanical properties of clay-based PVC polymer composite films. Polymers. 2023;15(8):1922.

